J Mater Sci (2009) 44:2271–2275
DOI 10.1007/s10853-008-3015-1

FESTSCHRIFT IN HONOUR OF PROF T R ANANTHARAMAN ON THE OCCASION OF HIS 80TH BIRTHDAY

Synthesis and characterization of cobalt–nickel alloy nanowires

S. Talapatra · X. Tang · M. Padi · T. Kim · R. Vajtai · G. V. S. Sastry · M. Shima · S. C. Deevi · P. M. Ajayan

Received: 1 May 2008 / Accepted: 22 September 2008 / Published online: 5 November 2008

Abstract We report on the synthesis and magnetic characterization of ordered arrays of cobalt–nickel alloy nanowires. These alloy nanowires were electrodeposited into the pores of anodic alumina templates. The physical properties of the samples were investigated using scanning electron microscopy, energy dispersive X-ray spectroscopy, transmission electron microscopy, and vibrating sample magnetometer. We found that for the alloy nanowires the field at which the magnetization saturates increases with increasing Co fraction and the saturation field in the normal direction is smaller than the parallel direction, indicating easy magnetization direction normal to wire axis. Nanowires with different compositional ratio of cobalt and nickel showed a nonlinear dependence of coercivity as a function of cobalt concentration. These findings will help tailor magnetic nanoalloys with controlled properties for various applications, such as high density magnetic storage or nanoelectrode arrays.

S. Talapatra (✉)
Department of Physics, Southern Illinois University Carbondale, Carbondale, IL 62901, USA
e-mail: stalapatra@physics.siu.edu
URL: www.physics.siu.edu/people/talapatra/index.html

X. Tang
Department of Physics, Applied Physics and Astronomy, Rensselaer Polytechnic Institute, Troy, NY 12180, USA

M. Padi · T. Kim · M. Shima · P. M. Ajayan
Department of Materials Science and Engineering, Rensselaer Polytechnic Institute, Troy, NY 12180, USA

R. Vajtai · M. Shima · P. M. Ajayan
Rensselaer Nanotechnology Center, Rensselaer Polytechnic Institute, Troy, NY 12180, USA

G. V. S. Sastry
Department of Metallurgy, Banaras Hindu University, Varanasi 221005, India

S. C. Deevi
RD&E Center Phillip Morris, Richmond, VA 23234, USA

Introduction

Magnetic materials at nanoscale possess unique properties due to their reduced dimensionalities [1–3]. The potential applications of magnetic nanostructures in a wide variety of future technologies have led to the study [1–8] of both the fundamental aspect of magnetism and their possible uses. Magnetic nanostructures have superior properties, as their bulk counterpart, which might be useful in developing them for microsensors, magnetoelectronics, and ultra-high-density magnetic storage devices. One of the advantages of using magnetic nanowire arrays as an ultra-high-density magnetic storage material is that recoding densities that can be achieved using these materials are much higher than those obtained in continuous magnetic film.

This factor itself provides enough impetus for studying the growth and properties of various magnetic nanowire systems. Due to these reasons, development of feasible techniques for fabrication of magnetic nanowires [3–15] has received a lot of attention recently. One of the most elegant and cost effective technique for growing nanowire arrays [9–17], is the electrodeposition of desired nanomaterials in nanoporous template materials. There are various nanoporous templates (ion track etched poly carbonate membrane, anodic alumina, etc.) which are used for electrodeposition of nanostructure materials [9–17]. However, using anodic alumina oxide (AAO) templates for nanowire deposition has its own advantages. The individual

nanopores in the AAO can be ordered into a close-packed honeycomb structure and the diameter of each pore and the separation between two adjacent pores can be controlled by changing the anodization conditions which in turns provides control over the structure of the nanowires [1, 9, 14]. The electrodeposited nanowires are generally dense, continuous, and extremely crystalline. In the past, a number of studies are dedicated to synthesize pure magnetic nanostructure such as pure cobalt [18, 19] and nickel [20, 21], magnetic multilayer, etc., using AAO templates. However, very few reports exist for growth and characterization of magnetic nanoalloys using this technique [16, 17]. Ferromagnetic alloys have potential for application in a variety of fields such as wear-resistant, corrosion-resistant, and/or heat-resistant materials, microelectronics, microsystems technology used to manufacture sensors and actuators, microrelays and ultra-high-density storage media [8, 16]. Developing functional materials from these alloys for different applications calls for controlled tailoring of these structures in terms of their dimensions, structures, and composition since these parameters will dictate their physical and magnetic properties. We report on the synthesis and characterization of cobalt–nickel alloy (CNA) nanowires. The advantage of Co Ni system is that its magnetic characteristics are dependent on cobalt concentration and it shifts from soft magnetic to permanent magnetic material with increasing cobalt fraction. In this article, we present our results on the fabrication and characterization of CNA nanowires. CNA nanowires with different compositional ratios were synthesized and their room temperature magnetic properties were investigated. The deposited nanowires were characterized using scanning electron microscopy (SEM), transmission electron microscopy (TEM), and energy dispersive X-ray spectroscopy (EDS). The magnetic properties of the nanowires were measured using a vibrating sample magnetometer (VSM) operating at room temperature.

Experimental

Electrodes for deposition were prepared by coating a thin layer of titanium (100 nm) and a layer of copper (1 μm) on one side of the alumina template (pore diameter ~250 nm) using electron-beam evaporation. This metal coating served as the contact for the template electrode. The metal/AAO assembly was attached to a copper tape (with the metal side in contact with the copper tape) and was covered with insulating tape such that a portion of the template is exposed. This assembly was used as one of the electrode for the electrodeposition. The electrodeposition was carried out using a classical three-electrode potentiostat system with an Ag/AgCl electrode as a reference electrode and a platinum wire as a counter electrode. An EG&G Princeton Applied Research potentiostat/galvanostat Model 273A was used to control the electrodeposition process. The electrolyte consisted of varying concentrations of cobalt sulfate ($CoSO_4 \cdot 7H_2O$) and nickel sulfate ($NiSO_4 \cdot 7H_2O$). For example for obtaining 55% CoNi nanowires we have used 5 g of $CoSO_4$, 30 g of $NiSO_4$, and 4.5 g of boric acid in 150 mL of water. CNA nanowires were grown potentiostatically. After the electrodeposition the AAO was etched using a 6 wt% sodium hydroxide solution to remove the template and expose the deposited alloy nanowires. The etched nanowires were washed and rinsed multiple times thoroughly with distilled water before performing SEM, and EDX analysis. The VSM measurements were performed on CNA nanowires before etching the alumina template.

Results and discussions

The results of the CNA nanowire growth are shown in Fig. 1. In Fig. 1a, SEM images of a large area of highly ordered vertical arrays of exposed nanowires with uniform structure is shown. This sample was etched using a 6 wt% NaOH solution for 10 min. The shorter etching time resulted in the exposure of only a small portion on the top of the CNA nanowires. The remaining part of the template helps in keeping a very stable assembly of the nanowires partially embedded in the AAO. In Fig. 1b, we present SEM image of CNA nanowires completely etched out from the AAO template. These nanowires are approximately 10 μm long and resulted from deposition which lasted for 1 h. The wires have diameters ~250 nm equal to the pore diameter of the AAO template used. The composition of the CNA nanowires was determined from EDS. A typical EDS spectra is shown in Fig. 1c. The intensity peaks for cobalt and nickel K and L lines are clearly visible in the spectra. This data were used to estimate the composition of these two metals present in the electrodeposited samples. The (data shown) nanowire alloys fabricated consisted of 54 at% of Co and 46 at% for Ni. For calculating the composition, we have used the intensity ratios of the cobalt and nickel K lines [22]. For checking the compositional consistency of the nanowires, EDS spectra for each of the samples were collected from multiple batches and the spectrum was acquired from different position along the length of the nanowire arrays.

The nanowire structures were further analyzed with TEM. For obtaining the diffraction pattern, the beam was focused such that it interacts mostly with the outer edge (cylindrical surfaces) of the nanowire. In this way, the beam was made to pass through the outer curvature of the

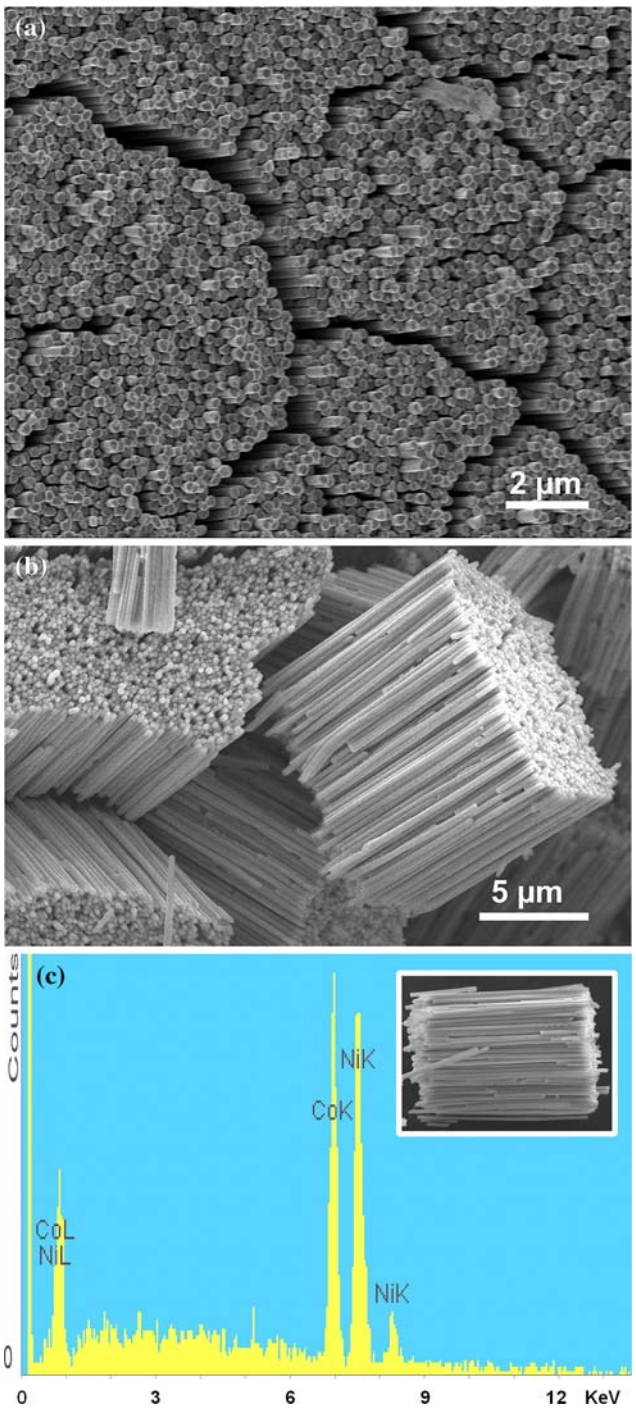

Fig. 1 SEM images of well-aligned arrays of cobalt nickel nanowires with varying length and diameters. **a** A large area showing alloy nanowire growth from the AAO. **b** Nanowire arrays completely etched out of the AAO templates showing typical length we achieved for one hour electrodeposition. **c** Energy dispersive spectra (EDS) showing the presence of cobalt and nickel. The Co and Ni K and L lines are clearly seen in the spectra. Inset shows the nanowire bundle from where the EDS were acquired

wires where the thickness is less as compared to the center of the nanowire. The results of one such TEM analysis is shown in Fig. 2. Figure 2a shows a low-magnification

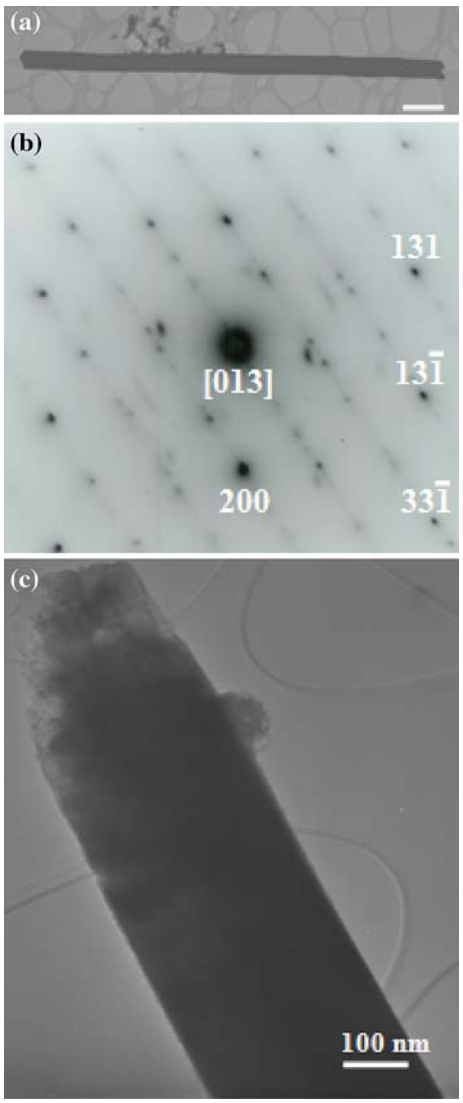

Fig. 2 High-resolution transmission electron microscopy of the nanowires **a** shows a low-magnification image of the nanowire showing uniform growth. **b** A typical pattern in [013] zone axis is shown. **c** A higher-magnification image of a typical rod is shown with visible microstructure at the nucleation and termination end of the rod

image of the nanowire showing uniform growth that prevailed in the electrolytic cell. A higher-magnification image of a typical rod shows the termination ends of the rods, which can be recognized by the uniformity of cross section and the visibility of the microstructure (Fig. 2b). Diffraction patterns obtained from one end to the other of the rod were found to vary in their zone axis indicating the polycrystalline nature of the rod. Together, they could be indexed on the basis of an f.c.c. lattice of a single phase. A typical pattern in [013] zone axis is shown in Fig. 2c. The phase could be identified as a solid solution of Co and Ni with a lattice parameter of 0.33 nm. This value of lattice parameter is close to that reported for Co–Ni solid solutions. The nets formed by intense reflections were used for

the indexing of the diffraction patterns on the basis of an f.c.c phase. In addition to these, one notices the presence of finely spaced spots along certain reciprocal lattice vectors suggestive of a superlattice formation. There is a varied opinion about the occurrence of superlattice structure in Co–Ni solid solutions in the literature [23]. At present, this aspect is under further study.

For magnetic characterization, we have used a VSM (Lake Shore, Model No. VSM 7407) operating at room temperature. Figure 3 shows the room temperature magnetic measurements on cobalt–nickel nanowire arrays having different cobalt fraction. Some of the observations that are clear from these magnetic measurements are the following. The hysteresis loops show strong magnetic anisotropy. With increasing Co fraction, the field at which the magnetization saturates increases. The saturation field in the normal direction is smaller than the parallel direction, indicating easy magnetization direction normal to wire axis. This observation is intriguing since considering only the shape anisotropy of the nanowires, the easy direction of magnetization should be parallel to the wire axis. The saturation field in the normal to wire direction is smaller than that in the parallel to wire direction, indicating an easy magnetization direction normal to wire axis, a result of the competition between the dipole interaction and shape anisotropy [24]. Previous work has shown [25] that, there is a strong dipolar field when the field is applied normal to the wire axis, while the dipolar interaction with field applied along the wire axis is too weak to be taken into account. Therefore, when the field is applied normal to the wire axis, the dipole field to any wire from neighboring wires is in the same direction as external field, thus a smaller field is needed to saturate the magnetization. There could be other possibilities too. For example, the TEM image in Fig. 2b shows diffraction pattern with streaks. The streaking effect generally manifests the presence of faults in the nanowires. Further, the wires could be textured (verification of the textures or the faults in the nanowires is beyond the scope of this work) and therefore can effect the magnetic properties of the alloy nanowires. In Fig. 3c, we present the dependence of the coercivity values for the nanowires with different cobalt concentration for field applied parallel and perpendicular to the wires. The electrodeposited Co–Ni nanowires exhibited a decrease in coercivity with increasing Co content up to approximately 55 wt.% for field applied parallel to the wire. Higher Co content resulted in an increase in coercivity. Similar dependence of coercivity as a function of cobalt concentration was also recently observed for electrodeposited Co–Ni thin films [26]. For fields applied perpendicular to the nanowires, the coercivity decreases for cobalt concentration up to 55 wt%. For higher concentration of Co, we did not observe any systematic trend. One possible explanation for this kind of behavior could be the formation of multidomains in the Co–Ni system with cobalt concentration <55 wt% which degrades the coercivity. For

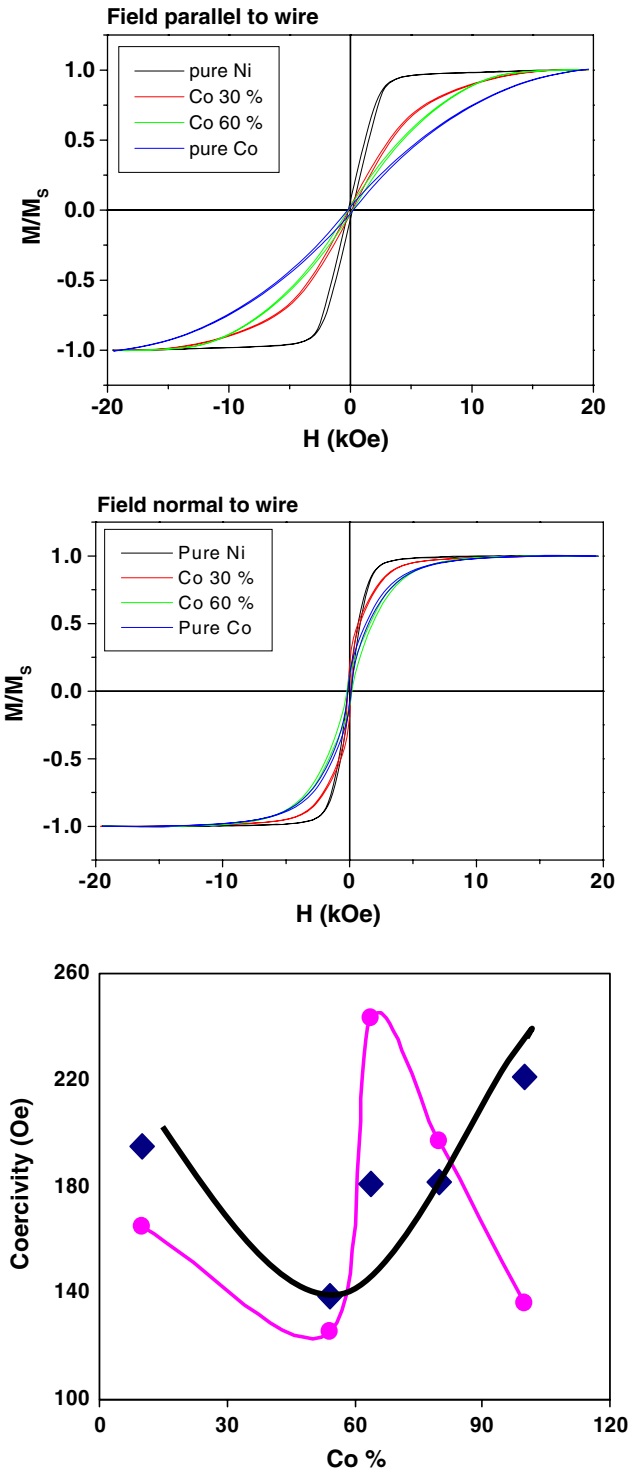

Fig. 3 The variation of the magnetic moment as a function of the magnetic field applied **a** parallel and **b** perpendicular to the axis of the nanowires is shown for nanowires with different Co concentration. **c** Variation of coercivity observed with varying cobalt concentration for nanowires with diameter of 250 nm

higher concentration of cobalt, many factors come into play. For example, the crystal structure of Co–Ni alloys changes from f.c.c. to h.c.p for Co concentration greater than 80 wt%. This could lead to the formation of single domain structure which can result in higher coercivites.

Conclusions

In conclusion, we have fabricated ordered arrays of magnetic alloy nanowires with controlled composition. We have shown that by using an electrochemical route magnetic alloy nanowires can be electrodeposited from a single electrodeposition bath by applying a single potential. This process produces nanowires with compositional controllability. The fact that the magnetic nanowires with tunable properties can be produced using a very simple method will help in developing/opening avenues for further research regarding lot of applications [26, 27] based on magnetic alloy nanostructures in a variety of fields such as high density magnetic storage [28], nanoelectrode arrays [20, 29, 30].

Acknowledgements PMA and RV acknowledge funding support from the RPI Nanoscale Science and Engineering Initiative of the National Science Foundation under NSF award numbers DMR-0117792 and DMR-0642573 on directed assembly of nanostructures and Philip Morris USA. The authors acknowledge Prof. G.W. Meng and Dr. Y.Y. Jung for helpful discussion. ST acknowledge financial support provided by SIUC ORDA through start-up funds.

References

1. Fert A, Piraux L (1999) J Magn Magn Mater 200:338. doi:10.1016/S0304-8853(99)00375-3
2. Skomski R, Zeng H, Sellmyer DJ (2002) J Magn Magn Mater 249:175. doi:10.1016/S0304-8853(02)00527-9
3. Allwood DA, Vernier N, Xiong G, Cooke MD, Atkinson D, Faulkner CC et al (2002) Appl Phys Lett 81:4005. doi:10.1063/1.1523634
4. Prinz GA (1999) J Magn Magn Mater 200:57. doi:10.1016/S0304-8853(99)00335-2
5. Nait Abdi A, Buchera JP (2003) Appl Phys Lett 82:430. doi:10.1063/1.1539908
6. Peng Y, Shen T-H, Zhao XG, Ashworth B, Faunce CA, Liu YW (2003) Appl Phys Lett 83:362. doi:10.1063/1.1590427
7. Saib A, Vanhoenacker-Janvier D, Huynen I, Encinas A, Piraux L, Ferain E et al (2003) Appl Phys Lett 83:2378. doi:10.1063/1.1610798
8. Sunder RS, Deevi SC (2005) Int Mater Rev 50:1. doi:10.1179/174328005X14302
9. Whitney TM, Jiang JS, Searson PC, Chien CL (1993) Science 261:1316. doi:10.1126/science.261.5126.1316
10. Hulteen JC, Martin CR (1997) J Mater Chem 7:1075. doi:10.1039/a700027h
11. Schwarzacher W, Attenborough K, Michel A, Nabiyouni G, Meier JP (1997) J Magn Magn Mater 165:23. doi:10.1016/S0304-8853(96)00465-9
12. Schonenberger C, van der Zande BMI, Fokkink LGJ, Henny M, Schmid C, Krulger M, Bachtold A, Huber R, Birk H, Staufer U (1997) J Phys Chem B 101:5497. doi:10.1021/jp963938g
13. Huczko A (2000) Appl Phys (Berl) A70:365
14. He H, Tao NJ (2004) In: Nalwa HS (ed) Encyclopedia of nanoscience and nanotechnology, vol X. American Scientific Publishers, San Diego, pp 1–18
15. Shankar KS, Kar S, Raychaudhuri AK, Subbannab GN (2004) Appl Phys Lett 84:993. doi:10.1063/1.1646761
16. Zhu H, Yang S, Ni G, Yu D, Du Y (2001) Scripta Mater 44:2291. doi:10.1016/S1359-6462(01)00761-8
17. Piercea JP, Plummer EW, Shen J (2002) Appl Phys Lett 81:1890. doi:10.1063/1.1506185
18. Yin AJ, Li J, Jian W, Bennett AJ, Xu JM (2001) Appl Phys Lett 79:1039. doi:10.1063/1.1389765
19. Garcia JM, Asenjo A, Velazquez J, Garcia D, Vazquez M, Aranda P et al (1999) J Appl Phys 85:5480. doi:10.1063/1.369868
20. Nielsch K, Wehrspohn RB, Barthel J, Kirschner J, Gosele U, Fischer SF et al (2001) Appl Phys Lett 79:1360. doi:10.1063/1.1399006
21. Nielsch K, Wehrspohn RB, Barthel J, Kirschner J, Fischer SF, Kronmuller H et al (2002) J Magn Magn Mater 249:234. doi:10.1016/S0304-8853(02)00536-X
22. Feldman LC, Mayer JW (1986) Fundamentals of surface and thin film analysis. Prentice Hall Inc., USA
23. Hnilicka M, Karmazin L (1974) Scripta Meter 8:1029. doi:10.1016/0036-9748(74)90404-9
24. Tang XT, Wang GC, Shima M (2006) J Magn Magn Mater 309:188. doi:10.1016/j.jmmm.2006.06.032
25. Zhan Q-F, Gao J-H, Liang Y-Q, Di N-L, Cheng Z-H (2005) PRB 72:024428. doi:10.1103/PhysRevB.72.024428
26. Kim D, Park D-Y, Yoo BY, Sumodjo PTA, Myung NV (2003) Electrochim Acta 48:819. doi:10.1016/S0013-4686(02)00773-9
27. Sapp SA, Mitchell DT, Martin CR (1999) Chem Mater 11:1183. doi:10.1021/cm990001u
28. Yu S, Li N, Wharton J, Martin CR (2003) Nano Lett 3:815. doi:10.1021/nl0340576
29. Menon VP, Martin CR (1995) Anal Chem 67:1920. doi:10.1021/ac00109a003
30. Forrer F, Schlottig F, Siegenthaler H, Textor M (2000) J Appl Electrochem 30:533. doi:10.1023/A:1003941129560